Journal of Virology

Virology | Full-Length Text

Functional characterization of *Microplitis demolitor* bracovirus genes that encode nucleocapsid components

Ange Lorenzi,[1] Michael J. Arvin,[1] Gaelen R. Burke,[1] Michael R. Strand[1]

AUTHOR AFFILIATION See affiliation list on p. 19.

ABSTRACT Bracoviruses (BVs) are endogenized nudiviruses in parasitoid wasps of the microgastroid complex (order Hymenoptera: Family Braconidae). BVs produce replication-defective virions that adult female wasps use to transfer DNAs encoding virulence genes to parasitized hosts. Some BV genes are shared with nudiviruses and baculoviruses with studies of the latter providing insights on function, whereas other genes are only known from nudiviruses or other BVs which provide no functional insights. A proteomic analysis of *Microplitis demolitor* bracovirus (MdBV) virions recently identified 16 genes encoding nucleocapsid components. In this study, we further characterized most of these genes. Some nucleocapsid genes exhibited early or intermediate expression profiles, while others exhibited late expression profiles. RNA interference (RNAi) assays together with transmission electron microscopy indicated *vp39*, *HzNVorf9-like2*, *HzNVorf93-like*, *HzNVorf106-like*, *HzNVorf118-like*, *and 27b* are required to produce capsids with a normal barrel-shaped morphology. RNAi knockdown of *vlf-1a*, *vlf-1b-1*, *vlf-1b-2*, *int-1,* and *p6.9-1* did not alter the formation of barrel-shaped capsids but each reduced processing of amplified proviral segments and DNA packaging as evidenced by the formation of electron translucent capsids. All of the genes required for normal capsid assembly were also required for proviral segment processing and DNA packaging. Collectively, our results deorphanize several BV genes with previously unknown roles in virion morphogenesis.

IMPORTANCE Understanding how bracoviruses (BVs) function in wasps is of broad interest in the study of virus evolution. This study characterizes most of the *Microplitis demolitor* bracovirus (MdBV) genes whose products are nucleocapsid components. Results indicate several genes unknown outside of nudiviruses and BVs are essential for normal capsid assembly. Results also indicate most MdBV tyrosine recombinase family members and the DNA binding protein *p6.9-1* are required for DNA processing and packaging into nucleocapsids.

KEYWORDS parasitoid, virus, *Microplitis demolitor*, bracovirus, endogenous virus element, nucleocapsid

Integration of all or portions of a viral genome into the germline of multicellular animals is referred to as endogenization (1, 2). Most endogenous virus elements decay under neutral evolution, but some persist and a few have been coopted for new functions (3, 4). Most known examples of cooption involve single genes or short sequences of viral origin (4). Prominent exceptions to this trend are the domesticated endogenous viruses (DEVs) in insects called parasitoid wasps (order Hymenoptera), which lay eggs in other insects that serve as hosts for offspring (5). DEVs from different virus ancestors have been identified in four parasitoid lineages (5, 6). Each consists of many genes from the virus ancestor, which interact to produce enveloped nucleocapsids containing DNA or virus-like particles (VLPs) with no nucleic acid (5, 6).

Editor Colin R. Parrish, Cornell University Baker Institute for Animal Health, Ithaca, New York, USA

Address correspondence to Michael R. Strand, mrstrand@uga.edu.

The authors declare no conflict of interest.

See the funding table on p. 19.

Received 30 May 2023
Accepted 19 September 2023

Published 25 October 2023

Through evolutionary convergence, wasps in each DEV-hosting lineage have coopted these virions or VLPs for a new essential function: transfer of virulence factors to hosts that enable wasp offspring to develop (5). The largest DEV-associated lineage evolved ~100 million years ago from a virus in the family *Nudiviridae* that integrated into the germline of a parasitoid in the family Braconidae (7–10). Speciation events have since given rise to a hyperdiverse, monophyletic assemblage (~50,000 spp.) of braconids named the microgastroid complex with DEVs named bracoviruses (BVs) (11).

Understanding of BV evolution derives from comparative studies of the *Nudiviridae*, its sister family the *Baculoviridae*, and microgastroid wasp species like *Microplitis demolitor*, *Cotesia congregata*, *Chelonus inanitus*, and *Chelonus insularis* that produce *Microplitis demolitor* Bracovirus (MdBV), CcBV, CiBV, and CinsBV respectively (8, 12–17). All nudiviruses and baculoviruses infect insects or other arthropods (14, 15). Viruses in both families have large circular, double-stranded (ds) DNA genomes (80–230 kb), usually replicate in the nuclei of several host cell types, and produce virions comprised of one or more nucleocapsids that are surrounded by a single envelope (14, 15). Baculoviruses and nudiviruses also share 21 core genes: *dnapol* and *helicase* (DNA replication); *lef-4, lef-8, lef-9, p47* (subunits of the RNA polymerase that transcribes viral genes); *lef-5* (initiation factor), *38K, p33, p6.9, vlf-1, vp39* (DNA packaging, virion production and assembly); *pif-0* (subsequently referred to as *p74*)-*pif-6, pif-8* (infectivity); and *Ac81* (14, 15). BV virions are morphologically similar to nudiviruses but differ in that they only replicate in the nuclei of calyx cells, which reside in the ovaries of female wasps (5, 15, 18, 19). Sequencing and genome assembly of *M. demolitor*, *C. congregata*, and *C. insularis* show that BV genomes consist of two components: (i) genes with known or hypothesized functions in producing virions and (ii) covalently closed, double-stranded DNAs encoding virulence genes that are packaged into capsids (12, 13, 16, 17). The former includes all of the core genes nudiviruses and baculoviruses share except *dnapol* and *ac81* plus other genes that are only known from nudiviruses or other BVs (12, 16, 17). Location of these genes in the genomes of sequenced wasps differ, but all are specifically transcribed in calyx cells before or during virion morphogenesis (5, 12, 13, 16, 17). Many of these genes are also single copy, but others have diversified into multimember families (12, 16, 17). The DNAs that are packaged into capsids derive from domains in the genomes of wasps called proviral segments. Proviral segments remain integrated but are amplified and processed in calyx cells during virion morphogenesis into circular (episomal) dsDNAs before packaging into capsids (5, 12, 16–22). The number of proviral segments and inventory of virulence genes they encode varies among BVs but flanking domains with functions in amplification and processing are conserved (5, 12, 16, 17, 21, 22). Female wasps inject eggs and virions into hosts that are primarily larval-stage moths (19). Eggs hatch into larvae while virions infect different cells, followed by the expression of virulence genes that alter growth and protect wasp progeny from host immune defenses (19). In contrast, BVs cannot replicate in hosts because none of the genes required to produce them reside on the DNAs that are packaged into virions. Thus, BV genome components can only be transmitted vertically (5, 19).

We previously developed RNA interference (RNAi) methods that specifically knockdown the expression of BV genes in wasps 80–95% with a corresponding loss of protein (18, 20). RNAi coupled with other assays in *M. demolitor* indicates several MdBV genes shared with baculoviruses and nudiviruses retain conserved functions including the subunits of the RNA polymerase and several envelope components (20, 23). Proteomic analysis of MdBV virions additionally identifies 16 genes encoding proteins that are exclusively or preferentially detected in nucleocapsids (23). Four of these are shared among baculoviruses, nudiviruses, and BVs (*vp39*, *vlf-1a*, *vlf-1b-1*, and *vlf-1b-2*), eight are shared with nudiviruses and other BVs (*int-1*, *HzNVorf9-like-1* and *-2*, *HzNVorf93-like*, *HzNVorf106-like*, *HzNVorf118-like*, *HzNVorf128-like,* and *27b*), and four are only known from other microgastroid wasps but exhibit features suggesting they derive from the nudivirus ancestor of BVs (*K425_459*, *35a-4*, *35a-5*, and *35a-13*) (8, 12, 13, 16, 17). In baculoviruses, VP39 is a structural capsid protein, while VLF-1 is classified as a

tyrosine site-specific recombinase on the basis of shared homology with family members from prokaryotes, eukaryotes, and viruses that infect prokaryotes (14). Genes named *int*, *HzNVorf140*, or *HzNVorf140-like* in nudiviruses and BVs also encode tyrosine site-specific recombinase family members (8, 10, 12, 15–17). In contrast, the other MdBV genes encoding nucleocapsid components share no significant homology to guide functional predictions.

In this study, we further characterized all of the single-copy genes encoding MdBV nucleocapsid components except *HzNVorf128*. We also conducted studies on all of the VLF and INT family members detected in nucleocapsids plus INT-2, which is not detected in nucleocapsids but is transcribed in calyx cells during virion morphogenesis (23). We included only one of the *35*a (*35*a-5), and *HzNVorf9-like* family members (*HzNVorf9-like-2*) in the study to manage the total number of genes examined. *M. demolitor* encodes two *p6.9* paralogs (*p6.9-1* and *-2*), which our previous proteomic studies did not detect in virions (20, 23) but in baculoviruses is a single-copy core gene encoding a DNA-binding protein that is required for genome packaging (24–26). Small size and arginine-serine richness hinders detection of P6.9 in proteomic data sets but reanalysis of earlier data (23) using other search programs detected P6.9-1 but not P6.9.2 in nucleocapsids. For each of the genes that were included in the study, we first assessed transcript abundance in ovaries during the late larval, pupal, and early adult stage relative to the known timing of other MdBV genes and virion morphogenesis. We then conducted functional assays by knocking down each gene by RNAi. Transmission electron microscopy (TEM) studies were used to assess the effects of knockdown on capsid assembly, virion morphogenesis, and packaging of processed proviral segments into virions. qPCR assays were used to measure the effects of knockdown on amplification and processing of proviral segments. Fig. S1 summarizes the overall design of the study. We report that some MdBV genes encoding nucleocapsid components exhibit early gene expression profiles while others exhibit intermediate or late gene expression profiles. RNAi-based studies indicated *vp39* and several other single-copy genes shared with nudiviruses and other BVs are required for capsid assembly, while all of the tyrosine site-specific recombinase family members except *int-2,* and *p6.9-1* are required for proviral segment processing and packaging of resulting DNAs into capsids.

RESULTS

MdBV nucleocapsid components derive from both early and late genes

M. demolitor emerges from its host, *Chrysodeixis includens*, as a larva (fourth instar) that spins a cocoon and pupates 28–30 h post-emergence (stage 1). After a 3-day pupal period [stage 2, 30–54 h post-emergence (day 1 pupa), stage 3, 54–78 h post-emergence (day 2 pupa), stage 4, and 78–102 h post-emergence (day 3 pupa)], the adult emerges and exits the cocoon (27, 28). The transcriptional cascade that regulates formation of MdBV virions in ovary calyx cells begins with upregulation of genes like the RNA polymerase subunits (*lef-4*, *lef-8*, *lef-9*, and *p47*) at the end of stage 1 when the female larva pupates, which is followed by upregulation of late core genes like previously studied envelope components [*pif-1, p74, MdBVe46 (=HzNVorf64*-like)] by stage 3 (day 2 pupa) (20, 23). Thus, MdBV genes are classified as early or late on the basis of when, post-emergence from the host, transcript abundance significantly increases in ovaries (20). MdBV virions are also first observed in calyx cells at stage 3, but early and late genes continue to be transcribed and virions continue to be produced during stage 4 (day 3 pupa) and for several days after females emerge as adults. We thus began this study by profiling the expression of MdBV genes encoding nucleocapsid components. Comparison to known early genes (*lef-4* and *lef-9*) indicated one of the MdBV tyrosine recombinase family members (*vlf-1a*) exhibited an early gene expression profile as evidenced by transcript abundance already being elevated in ovaries at the end of stage 1 (=24 h post-emergence from the host). However, the other tyrosine recombinase family members whose products are detected in nucleocapsids (*vlf-1b-1*, *vlf-1b-2*, and *int-1*) and *p6.9-1* exhibited intermediate or late gene expression patterns with transcripts

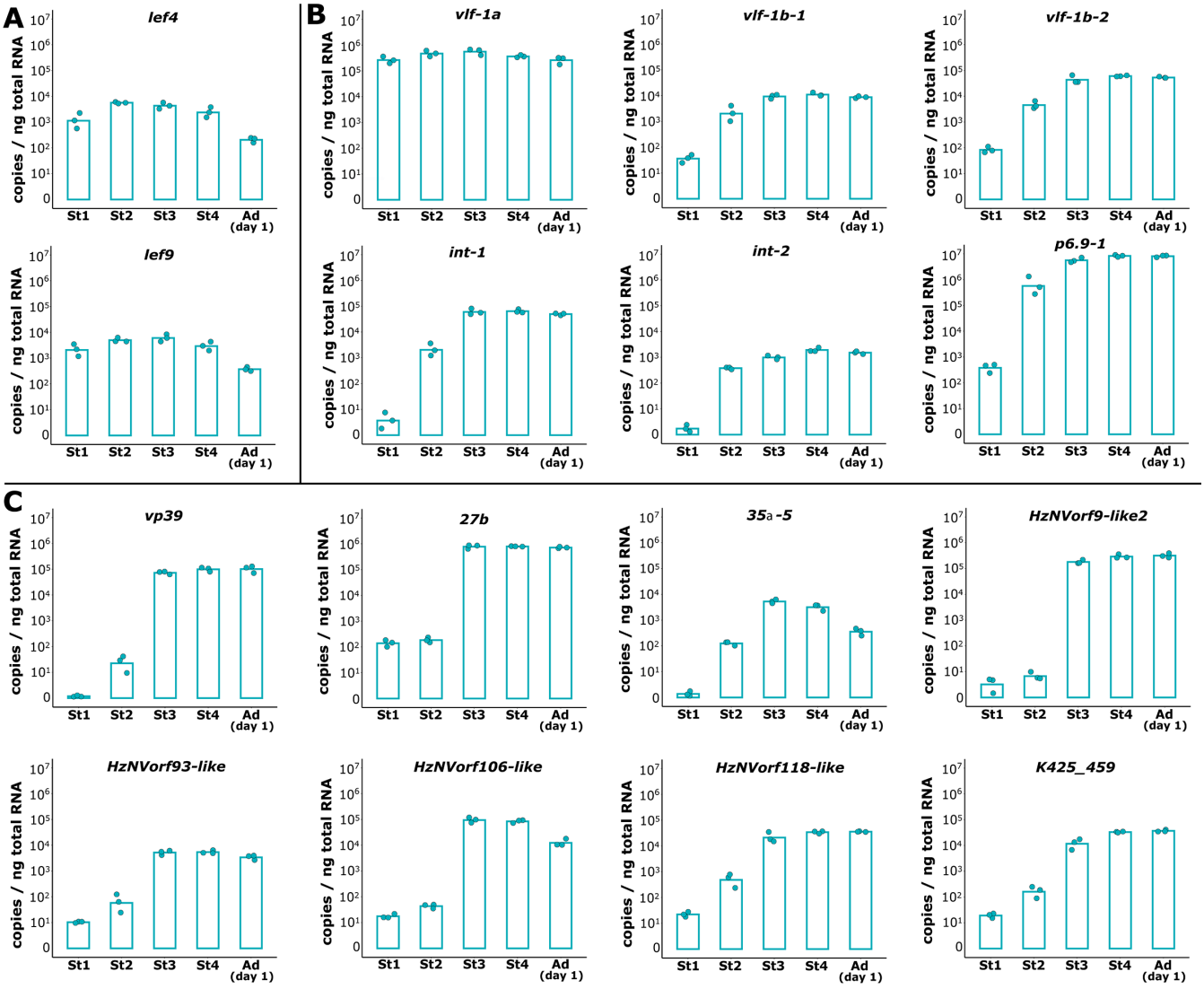

FIG 1 Transcript abundance of MdBV genes in ovaries from *M. demolitor* females. Ovaries collected from stage 1–4 pupae (St 1–4) or day 1 adults were processed for RT-qPCR assays. (A) *lef-4* and *lef-9* (controls) that were previously classified as early genes (20). (B) Tyrosine site-specific recombinase family members identified to encode nucleocapsid components (*vlf-1a*, *vlf-1b-1*, *vlf-1b-2*, and *int-1*) plus *int-2* and *p6.9-1* exhibit expression patterns that classify them as early or intermediate genes. (C) Other genes identified to encode nucleocapsid components (*vp39*, *27b*, *35a-5*, *HzNVorf9-like2*, *HzNVorf93-like*, *HzNVorf106-like*, *HzNVorf118-like*, and *K425_459*) exhibit expression patterns that classify them as late genes. For each graph, bars show the mean copy number for each transcript per ng of total RNA while solid circles show copy number for each biological replicate.

increasing to ~10^3 copies per ng of total RNA in ovaries at stage 2 (intermediate) or stage 3 (late) (Fig. 1A and B). *Int-2*, which is not detected in MdBV nucleocapsids (23), also exhibited an intermediate gene expression profile although transcript abundances were lower than for the other tyrosine recombinase family members (Fig. 1B). The remaining genes (*vp39*, *27b*, *35a-5*, *HzNVorf9-like2*, *HzNVorf93-like*, *HzNVorf106-like*, *HzNVorf118-like*, and *K425_459*) exhibited late expression profiles with transcript abundances remaining at low levels until increasing to 10^3 or more copies per ng of total RNA in stage 3 (Fig. 1C). Transcript abundances for all of the nucleocapsid-associated genes we profiled remained elevated in stage 4 (=day 3 pupae) and day 1 adults (=24 h post-eclosion) (Fig. 1).

Knockdown of most single-copy late genes results in formation of aberrant capsid-like structures

We expected that several genes encoding nucleocapsid components are required for normal capsid assembly. We therefore focused first on *vp39*, which as earlier noted encodes a nucleocapsid structural protein in baculoviruses, and most of the single-copy genes encoding nucleocapsid components that are only known from nudiviruses and/or other BVs. We injected specific dsRNAs corresponding to each of these genes into *M. demolitor* larvae after they emerged from the host and spun a cocoon (stage 1) (Fig. S1). We then assessed knockdown of each gene by isolating total RNA from ovaries of newly emerged adult females (day 1), which showed that transcript abundance of each gene was reduced by 90% or more when compared to control females injected with ds-*eGFP* (Fig. S2).

The calyx region in *M. demolitor* ovaries consists of calyx cells that increase in size proximally to distally with virion formation predominantly occurring in the nuclei of the largest, distal-most cells that are closest to the calyx lumen (27, 29, 30). Virion morphogenesis in these calyx cells progresses through four phases: (i) *de novo* appearance of spherical or comma-shaped envelopes, (ii) *de novo* appearance of barrel-shaped, electron-dense nucleocapsids in proximity to envelopes that are individually surrounded by envelopes to form virions, (iii) assembly of virions into parallel arrays, and (iv) disassembly of these arrays with virions fully filling the nucleus. Calyx cell lysis then results in release of virions into the calyx lumen (23, 27, 30). As noted above, MdBV envelopes, nucleocapsids, and virions are first observed in calyx cell nuclei at stage 3 (day 2 pupa) but as distally located calyx cells lyse and release mature virions into the lumen, morphogenesis begins in neighboring calyx cells which become the distal-most cells by the time they reach phase 4 and lyse. In this way, virions continue to be produced and released into the calyx lumen in day 3 pupae (stage 4) and in adults. We assessed the effects of knocking down different genes on capsid assembly and virion morphogenesis by using TEM to examine distally located calyx cells in the ovaries of day 1 adult females. Controls injected with ds-*eGFP* showed that virion morphogenesis progressed normally through four phases as presented in intermediate and high magnification TEM images with cartoons (Fig. 2A through D) and low magnification TEM images that show entire or near-entire calyx cells in phases 1–4 (Fig. S3A through D). The images shown in Fig. S3 further indicate the events shown in Fig. 2A through D occur over the entire nucleus.

We next compared virion morphogenesis in females treated with ds-*vp39*, which showed that knockdown had no effect on envelope formation (phase 1), but irregular-shaped structures formed *de novo* in phase 2 that envelopes individually surrounded suggesting these structures were morphologically abnormal capsids (Fig. 2E and F). Resulting virions accumulated in random orientation but thereafter did not assemble into parallel arrays (phase 3) before filling the nucleus and being released by cell lysis into the calyx lumen (Fig. 2G and H). RNAi knockdown of *HzNVorf9-like2*, *HzNVorf106-like*, or *HzNVorf118-like* also resulted in the formation of irregularly shaped capsids that envelopes surrounded to produce virions that were released into the calyx cell lumen (Fig. S4A through C).

Knockdown of *HzNVorf93-like* produced a different phenotype with envelopes forming normally followed by the *de novo* appearance of electron dense, granular aggregations of varying size that are in proximity to envelopes and barrel-shaped capsids that are electron dense or electron translucent (Fig. 3A and B). Capsids with no visible envelopes were present in most of the large and intermediate-size aggregations but small aggregations usually had no visible capsids (Fig. 3A and B). Some capsids in these aggregations were also electron dense suggesting the presence of packaged DNA while others were electron translucent suggesting an absence of DNA as occurs with the loss of several genes that disable DNA packaging in baculoviruses (14). Envelopes surrounded some of the small aggregations with no visible capsids but larger aggregations remained unenveloped (Fig. 3A through C). Envelopes with or without small aggregations or barrel-shaped capsids accumulated in calyx cells that also

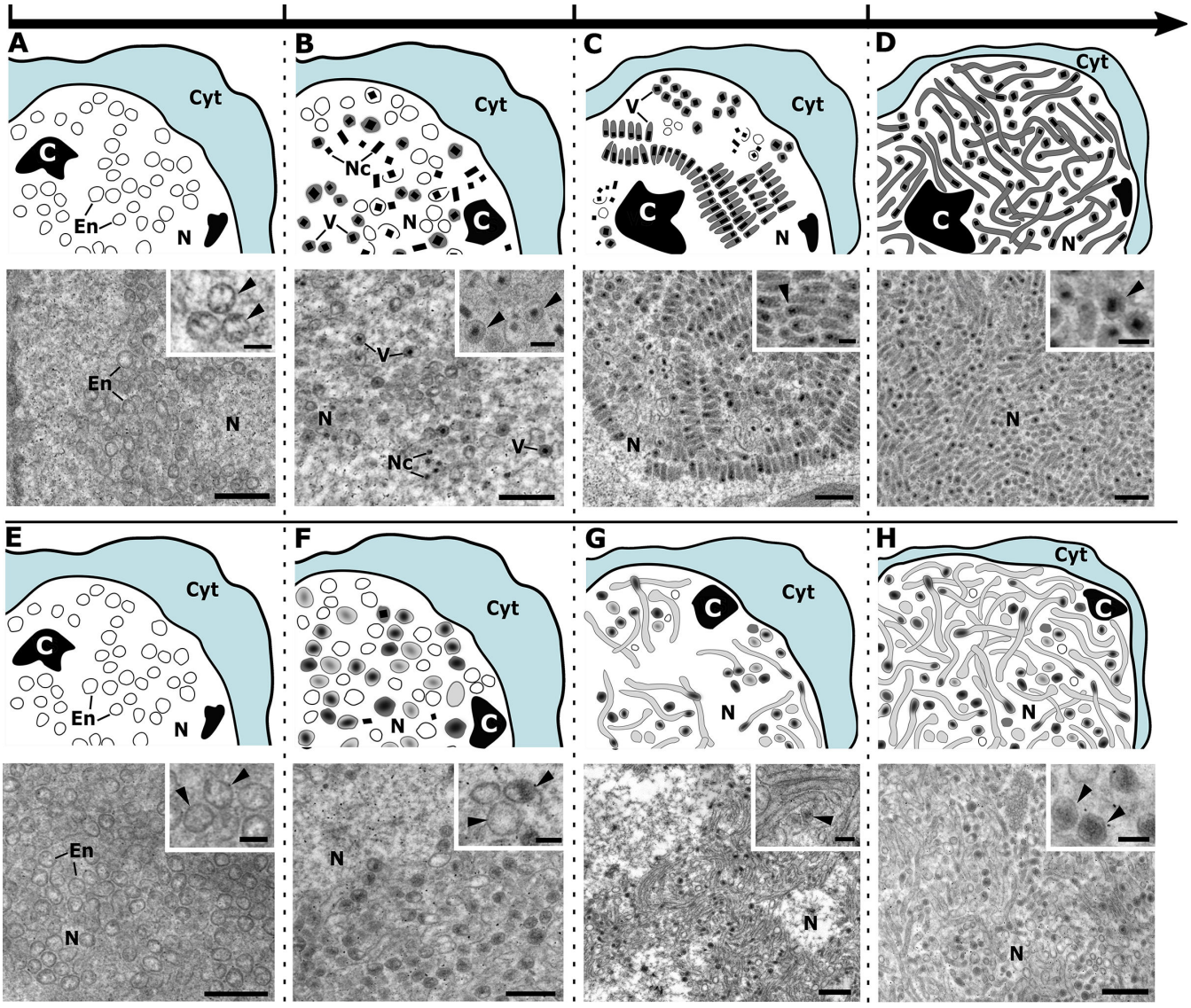

FIG 2 Virion morphogenesis (phases 1–4) in calyx cells from newly emerged adult females injected with ds-*eGFP* (control) (A–D) or ds-*vp39* (E–H). Upper panels show cartoons of a calyx cell nucleus at each phase, while the lower panel shows a corresponding TEM image at intermediate or high (insert) magnification (calyx cell cytoplasm (Cyt), calyx cell nucleus (N), MdBV envelope (En), MdBV nucleocapsid (Nc), MdBV virion (V), and chromatin (C). Also, see Fig. S3A through D showing low magnification TEM images of phases 1–4 calyx cells from control females, which correspond to the events illustrated in the cartoons. (A) Phase 1: *de novo* appearance of envelopes in the nucleus. Arrowheads highlight rounded envelopes in the insert image. (B) Phase 2: *de novo* appearance of electron dense, barrel-shaped nucleocapsids in proximity to envelopes. Envelopes in the process of surrounding nucleocapsids or that have surrounded nucleocapsids to produce virions are also present. Arrowheads in the insert image highlight newly formed virions. Also, note the presence of less electron dense material than inside capsids, which is present between the envelope and nucleocapsid. (C) Phase 3: virions in parallel arrays. Arrowhead in the insert image highlights a virion in sagittal orientation. (D) Phase 4: virions with elongated envelopes fill the nucleus, which is followed by calyx cell lysis. Arrowhead in the insert image highlights the anteriorly positioned nucleocapsid in an elongated envelope in cross section. (E and F) Phases 1–4 calyx cell nuclei from females injected with ds-*vp39*. Upper and lower panels with inserts as defined for (A–D). (E) Phase 1: *de novo* appearance of envelopes in *vp39* knockdown wasps. (F) Phase 2: *de novo* appearance of irregularly shaped capsids that envelopes surround. (G) Phase 3: envelopes without visible capsids and envelopes surrounding aberrant capsids that do not assemble into parallel arrays. (H) Phase 4: envelopes with and without aberrant capsids filling the nucleus. Scale bars for the intermediate magnification TEM images = 400 nm, scale bar for the higher magnification insert TEM images = 100 nm. The insert TEM images for each panel were selected to show envelopes, capsids, or virions at higher magnification. None come from a location within the TEM image shown at intermediate magnification.

lysed to release their contents into the calyx lumen. Knockdown of *27b* also resulted in envelopes forming normally in calyx cell nuclei, but this was followed by the appearance of structures with a spheroidal or corkscrew appearance (Fig. 3D and E). Envelopes

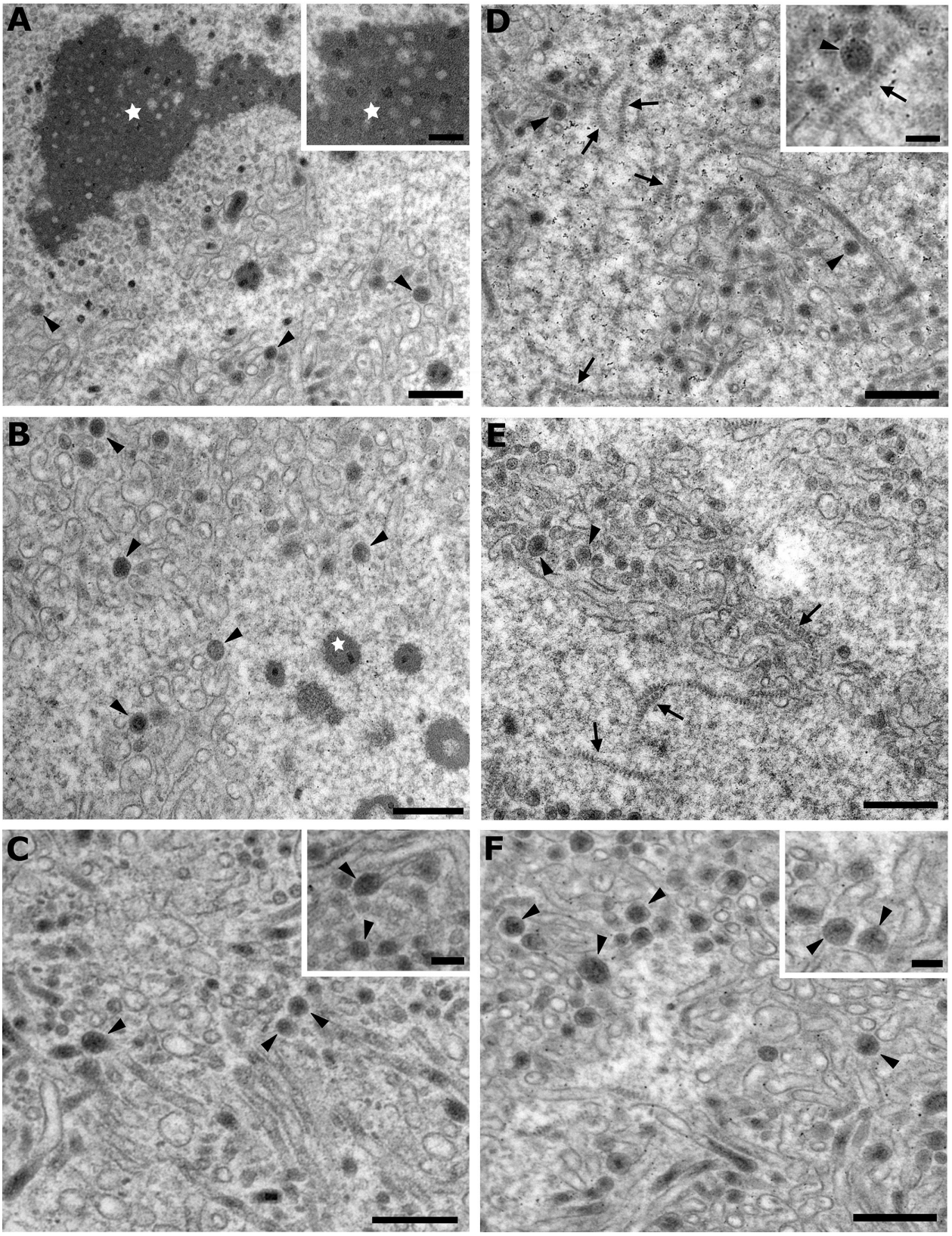

FIG 3 Virion morphogenesis in *HzNVorf93-like* or *27b* knockdown females. *M. demolitor* larvae were injected with ds-*HzNVorf93-like* or ds-*27b* followed by collection and processing of ovaries for TEM analysis. (A–C) Images from *HzNVorf93-like* knockdown females. (A) Image showing the presence of envelopes, capsids, and granular aggregations of varying size in a calyx cell nucleus (phase 2). The larger aggregation (star) contains several capsids in sagittal and

(Continued on next page)

FIG 3 (Continued)

cross-section that are electron dense or electron translucent with no visible envelope. Several of the intermediate size aggregations also contain capsids but the small aggregations do not. Insert image at higher magnification shows the larger aggregation with electron dense and electron translucent capsids present. (B) Image showing another region in the nucleus of a calyx cell (phase 2) with only intermediate and small aggregations present in proximity to envelopes. The intermediate-size aggregation (star) contains an electron dense capsid while the arrowheads highlight small aggregations with no visible capsids but are in several instances enveloped. (C) Lower and higher magnification images of a calyx cell nucleus showing envelopes or envelopes surrounding small aggregations that fully fill the nucleus (phase 4). Arrowheads in the insert image show enveloped small aggregations are anteriorly positioned. (D–F) Images of calyx cell nuclei from females injected with ds-*27b*. (D and E) show calyx cell nuclei with electron-dense spheroidal (arrowheads) and cork-screw structures (arrows) in proximity to envelopes (phase 2). Insert image in (D) shows higher spheroidal and corkscrew structures at higher magnification. (F) Lower and higher magnification images showing a calyx cell nucleus with empty envelopes or envelopes surrounding the electron-dense spheroidal structures (phase 4). Arrowheads show these electron-dense spheroidal structures are anteriorly positioned and have an elongate morphology in sagittal orientation. Scale bars for lower magnification images = 400 nm, scale bar for higher magnification insert images = 100 nm. The lower and higher magnification insert images in (C, D, and F) do not come from same location in the calyx cell that was photographed.

surrounded some of the spheroidal structures which together with empty envelopes filled the nucleus before calyx cells lysed (Fig. 3F). We selected only one (*35a-5*) of the three MdBV *35a* family members that are preferentially detected in nucleocapsids (23) for knockdown, which resulted in no visible defects in capsid morphology or virion morphogenesis when compared to control wasps injected with ds-*eGFP* (Fig. S5A). Knockdown of *K425-459* also had no effects on nucleocapsid morphology or virion formation when compared to control wasps (Fig. S5B).

Tyrosine site-specific recombinase family members form two clades in BVs and nudiviruses

Tyrosine site-specific recombinase family members are primarily known from prokaryotes, eukaryotes like some yeast, and viruses that infect prokaryotes (31). All share a ~180 amino acid catalytic domain, divided into two boxes, containing a largely conserved pentad (R-H-R-H/W-Y) that is required for catalyzing DNA strand breakage in well-studied family members like Cre and Flp (32). Biological processes regulated by different family members include integration and excision of DNAs from genomes, and the resolution of DNA dimers or multimers into monomers (32). Baculoviruses also encode one tyrosine site-specific recombinase family member, originally named very late factor 1 (*vlf-1*), which is detected in nucleocapsids (14), while BVs and nudiviruses encode two or more family members referred to as *vlf*, *int*, *HzNVorf140*, or *HzNVorf140-like* genes (10, 15, 17, 20). Before conducting any functional assays with the MdBV family members, we first compared tyrosine site-specific recombinases from nudiviruses, BVs, and the model baculovirus Autographa californica nucleopolyhedrovirus (AcMNPV) to one another. This showed that VLF-1 from AcMNPV contained an R-N-R-H-Y pentad (Fig. S6). Nudviruses in the genus *Alphanudivirus* and the one known isolate [*Tipula oleracea* nudvirus (ToNV)] classified as a *Deltanudivirus* encode two tyrosine site-specific recombinases named INT and VLF-1 (10, 15) (Fig. S6). INT in these genera contained an R-H-R-H-Y pentad while VLF-1 contained an R-N/T/Q/K-R-H-Y pentad. Gammanudiviruses encode one family member previously named INT with an R-H-R-H-Y pentad plus two family members named VLF-1 in which one contained an R-H/Q/K-R-H-Y pentad while the other is truncated (Fig. S6). The *Betanudivirus* currently consists of two isolates from the moth *Helicoverpa zea* (HzNV1 and HzNV2) which also encode one family member named INT with a conserved pentad (R-H-R-H-Y), VLF-1 with a largely conserved pentad (R-Q-R-H-Y) and a third family member HzNVORF140 with no recognizable pentad owing to multiple amino acid replacements (Fig. S6). Among BVs, MdBV encodes one family member named INT-1 with a conserved pentad (R-H-R-H-Y) and a second family member named VLF-1a with an R-K-R-H-Y pentad, whereas VLF-1b-1 is truncated, VLF-1b-2 lacks the essential tyrosine in position 5, and INT-2 has multiple replacements that result in loss of a recognizable catalytic pentad (Fig. S6). CcBV, CiBV, and CinsBV also encode two family members named INT (or INT-1) and VLF-1 with similar pentads as MdBV INT-1 and VLF-1, plus two or three other subfamily members named INT-2 or HzNVORF140-like

with truncations or replacements (Fig. S6). Altogether, most genes named INT have an R-H-R-H-Y pentad as found in tyrosine site-specific recombinases from a number of other organisms, whereas genes named VLF tend to have an R-X-R-H-Y pentad with X being H, N, T, Q, or K (Fig. S6). However, the remaining tyrosine site-specific recombinase family members in nudiviruses and BVs lack intact catalytic domains due to truncation or multiple amino acid replacements.

We assessed relatedness by using the full protein sequences highlighted in Fig. S6 to generate a maximum likelihood tree (Fig. 4). Results overall suggest that *vlf-1* duplicated in the ancestor of nudiviruses to generate *int*, which results in nudiviruses and BVs encoding two clades of tyrosine site-specific recombinases. That all nudiviruses and some BVs encode one *int* gene but other BVs (MdBV and CcBV) encode two strongly suggests the nudivirus ancestor of BVs encoded one *int* gene that later duplicated in the common ancestor of *M. demolitor* and *C. congregata*. Grouping of VLF-1 and VLF-1b/HzNVORF140-like sequences in BVs with high support, which are also separate from *Betanudivirus* HzNVORF140 family members, indicated each is a BV VLF paralog (Fig. 3). We further concluded that genes named *HzNVorf140* (nudiviruses) or *HzNVorf140-like* (BVs) belong to the VLF clade and should henceforth be named as such. The presence of two *vlf* paralogs in some nudiviruses raises the possibility that the BV ancestor also encoded two *vlf* genes. Alternatively, the most closely related nudivirus to BVs currently known is ToNV (10), which has only one *vlf* gene (named *vlf-1*) (Fig. S6). Thus, the two *vlf* genes some BVs encode most likely arose by duplication after endogenization of the ancestor, which was followed by a second duplication in the common ancestor of *M. demolitor* and *C. congregata*, that produced a third family member also lacking a conserved pentad (Fig. 3). Finally, since two genera of nudiviruses (*Betanudivirus* and *Gammanudivirus*) and all BVs maintain VLF paralogs that are truncated or have many amino replacements in the catalytic domain suggests these factors may not be functional tyrosine site-specific recombinases but have other activities.

Knockdown of most tyrosine site-specific recombinase family members and *p6.9-1* produces electron translucent nucleocapsids

Baculovirus VLF-1 may have roles in genome processing although exact functions remain unclear (14). However, deletion of *vlf-1* from AcMNPV also increases DNase sensitivity of the viral genome while producing electron translucent nucleocapsids which together suggest this gene is required for packaging of the DNA genome and/or the structural integrity of nucleocapsids (33, 34). Baculoviruses lacking *p6.9* also produce electron translucent nucleocapsids owing to its role as a DNA binding protein that condenses the viral genome which is also required for packaging into capsids (26). We previously reported that RNAi knockdown of MdBV *vlf-1a* increases DNase sensitivity of the circularized DNAs that are packaged into capsids after proviral segment processing, which is also associated with producing electron translucent nucleocapsids (20). However, we did not know at the time of this study that four family members are detected in nucleocapsids; two of which have conserved catalytic domains (VLF-1a and INT-1) and two do not (VLF-1b-1 and VLF-1b-2) (23). We also did not know the fifth family member lacking a catalytic domain (INT-*2*) is absent from nucleocapsids (23). We thus assessed the effects of individually knocking down each family member plus *p6.9-1* on packaging of processed DNAs into capsids by TEM (Fig. S1). RT-qPCR assays showed that gene-specific dsRNAs reduced transcript abundance of the targeted tyrosine site-specific recombinase family member but had no significant effect on transcript abundances of other family members indicating knockdown was specific (Fig. S7). RT-qPCR assays also indicated *p6.9.1* was successfully knocked down (Fig. S7). Knockdown of each tyrosine site-specific recombinase family member detected in capsids and *p6.9-1* resulted in formation of barrel-shaped capsids that did not differ from normal but were electron translucent which strongly suggested an absence of packaged DNA (Fig. 5A through E). In contrast, knockdown of *int-2* resulted in formation of electron-dense nucleocapsids and virions with a normal morphology (Fig. 5F).

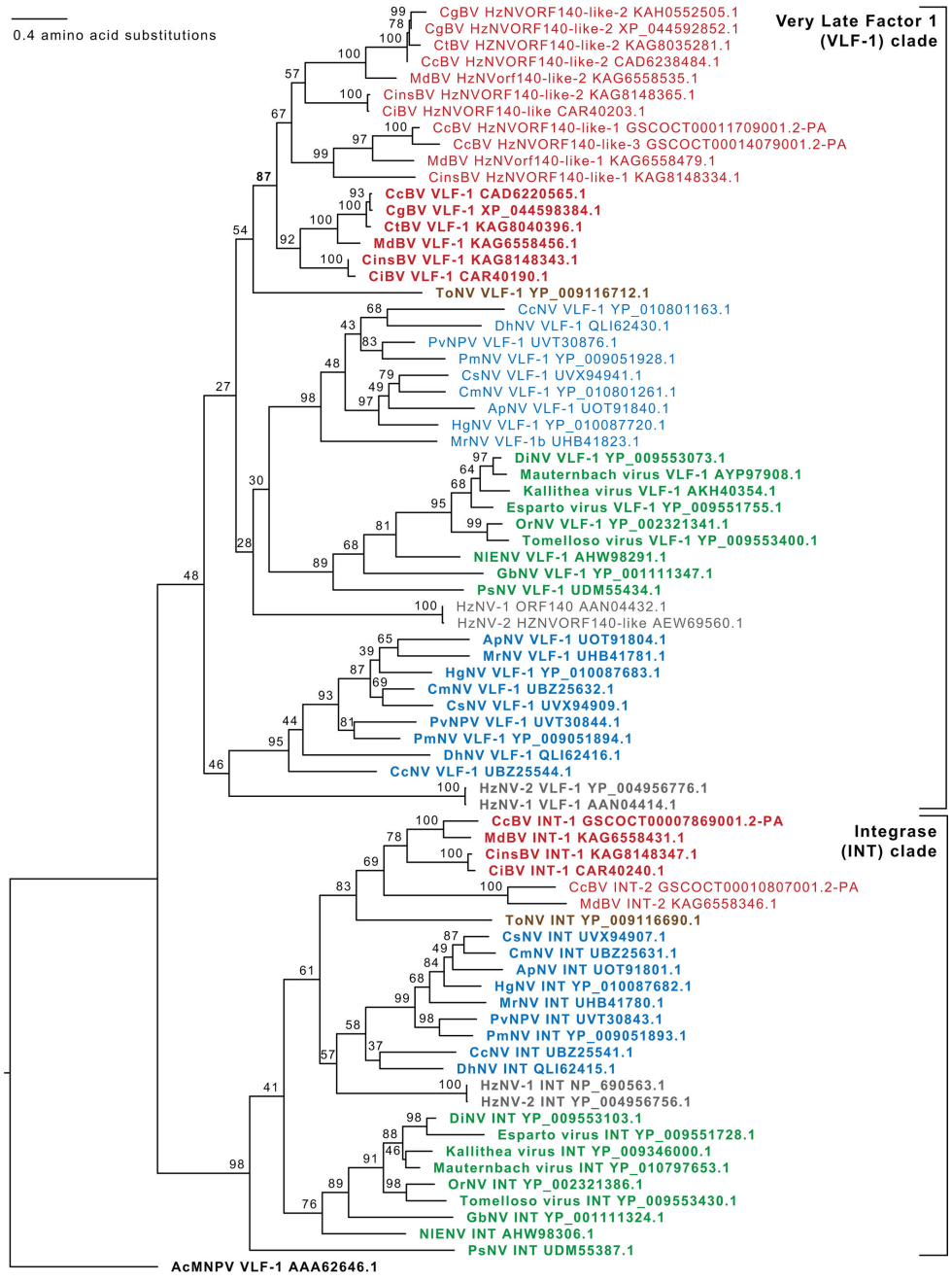

FIG 4 Maximum likelihood tree of tyrosine site-specific recombinase proteins from baculoviruses, nudiviruses, and bracoviruses. Virus types are indicated by color as described in Fig. S6. Proteins shown in bold type have R-X-R-H-Y pentads, while those in regular type are missing at least one of these residues due to truncation or replacements (see Fig. S6). Numbers located to the top left of nodes indicate bootstrap support. Taxon labels contain viruses, protein names, and accession numbers. Grouping overall indicates tyrsosine site-specific recombinases in BVs and nudiviruses form a VLF-1 clade consisting of proteins named in the literature as VLF-1, VLF-1a, VLF-1b, HzNVORF140, and HzNVORF140-like and an INT clade consisting of proteins named INT, INT1, or INT-2.

Knockdown of most tyrosine site-specific recombinases reduces proviral segment processing

A total of 25 MdBV proviral segments (A-X) reside in the *M. demolitor* genome in eight loci (12, 13). Loci plus flanking sequence are amplified as either head-to-tail (loci 3, 4, 6, and 8) or head-to-head/tail-to-tail concatemers (loci 1, 2, and 5) (22). Each intact

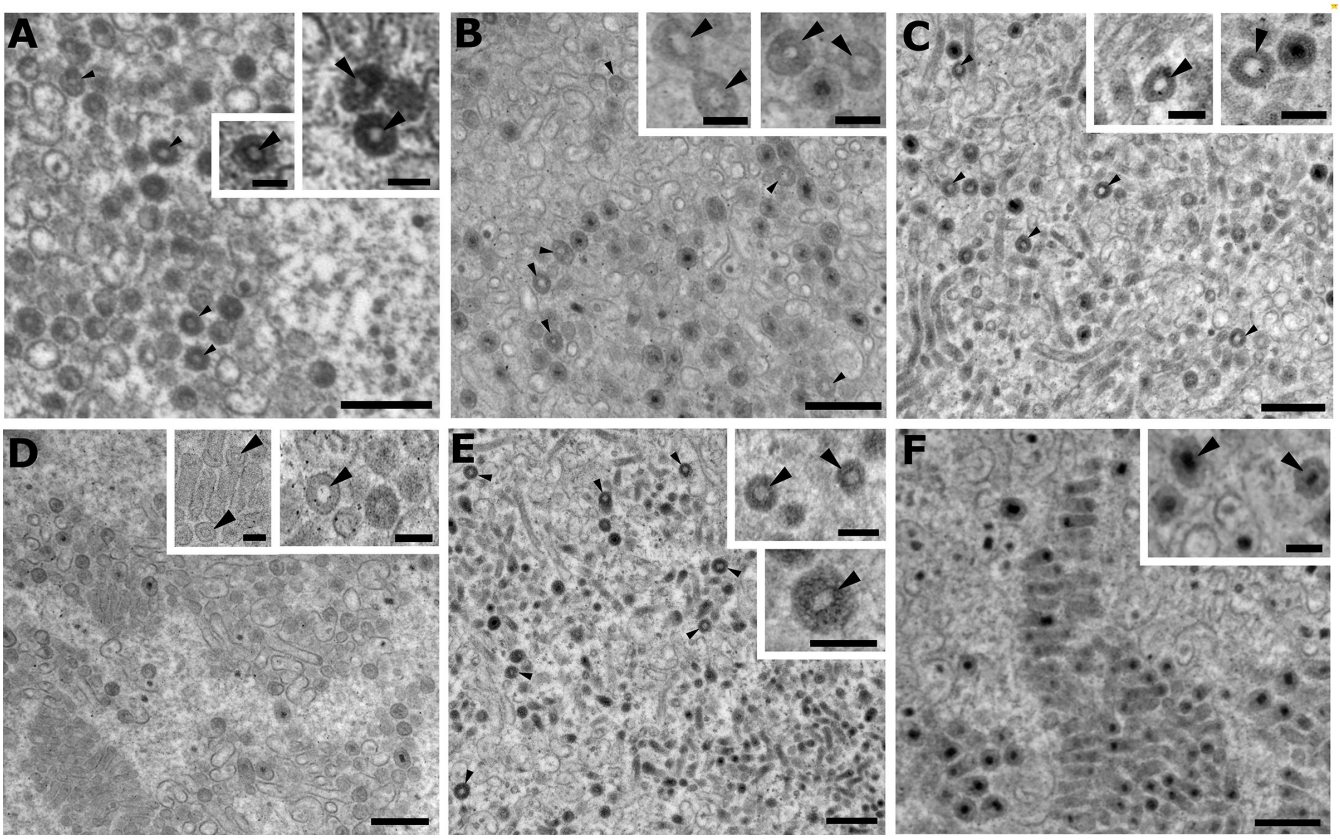

FIG 5 MdBV morphogenesis in *vlf-1a*, *vlf-1b-1*, *vlf-1b-2*, *int-1*, *int-2,* or *p6.9-1* knockdown females. *M. demolitor* larvae were injected with each dsRNA followed by collection and processing of ovaries for TEM analysis. (A–D) Images of cell nuclei from females injected with ds-*vlf-1a*, ds-*vlf-1b-1*, ds-*vlf-1b-2*, and ds-*int-1*, respectively. Each image shows virions consisting of a single envelope and a nucleocapsid. Most capsids are electron translucent which strongly suggests the absence of packaged DNA (arrowheads). Arrowheads in the higher magnification insert images further highlight that capsids are electron translucent but electron dense material is still present between the envelope and capsid. (E) Lower and higher magnification insert images of a calyx cell nucleus from a female injected with ds-*p6.9-1* showing most virions also contain electron translucent capsids. (F) Lower and higher magnification insert images of a calyx cell nucleus from a female injected with ds-*int-2* showing virions contain electron-dense nucleocapsids that morphologically do not differ from control females injected with ds-*eGFP* (see Fig. 2C). Abbreviations in the image are as defined in Fig. 2. Scale bars for lower magnification images = 400 nm, scale bar for higher magnification insert images = 100 nm. The lower and higher magnification insert images were selected to show the morphology of virions for each treatment and thus do not come from same location in the calyx cell that was photographed.

proviral segment is then processed by homologous recombination within conserved direct repeats, producing monomeric, and circularized dsDNAs that are individually packaged into virions plus rejoined flanking sequences (empty loci) from each replication unit that remain unpackaged (22, 29). We previously reported that RNAi knockdown of MdBV *vlf-1a* and *int-1* inhibits processing of proviral segment B which is in locus 1 (20). However, our finding that knockdown of each *vlf* and *int* family member except *int-2* produces electron translucent nucleocapsids prompted us to ask if each is also required for proviral segment processing despite only VLF-1 and INT-1 having catalytic domains. We thus knocked down each family member by RNAi and isolated genomic DNA from ovaries of newly emerged adult females (Fig. S1). We then used a qPCR assay that measured copy number of the intact and rejoined forms of two proviral segments that are amplified as head-to-tail concatemers [S (locus 6), J (locus 3)] and two proviral segments that are amplified as head-to-head/tail-to-tail concatemers [R (locus 5), V (locus 2)] (Fig. S8). If a given *vlf* or *int* family member is required for processing of these segments, knockdown would be expected to increase copy number of the intact form relative to control females treated with ds-*eGFP,* whereas copy number of the rejoined form would be reduced. Outcomes for each proviral segment were fully consistent with

this expectation for each family member that is detected in nucleocapsids (Fig. 6). Knockdown of *p6.9-1* also had the same effect (Fig. 6), but knockdown of *int-2* had no effect on intact or rejoined copy number for any of the proviral segments we examined

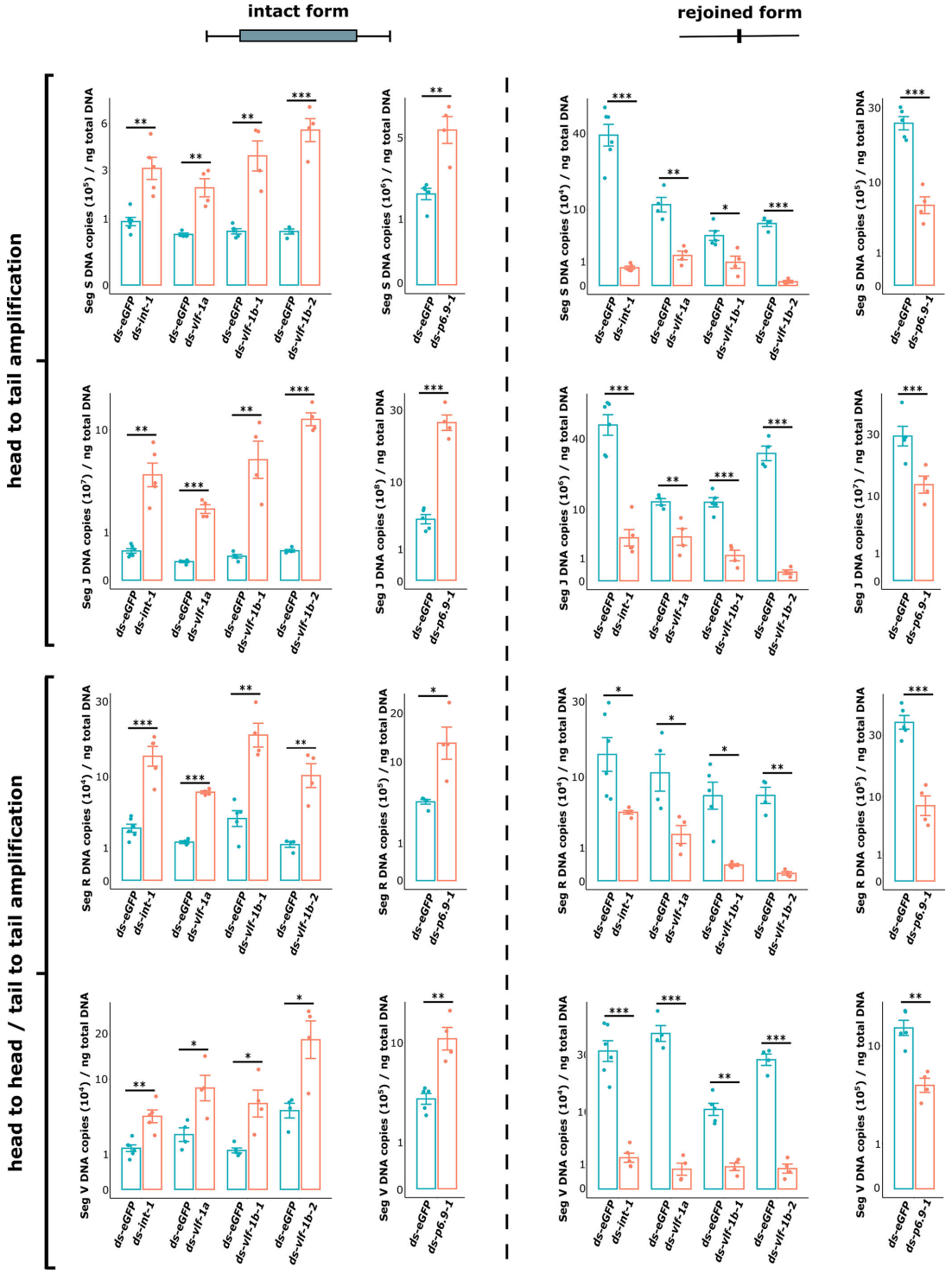

FIG 6 RNAi knockdown of MdBV tyrosine recombinase family members and *p6.9-1* alters processing of proviral segments S, J, R, or V. *M. demolitor* larvae were injected with double stranded RNA targeting *vlf1-a*, *vlf1b-1*, *vlf1b-2*, *int-1*, or *p6.9-1*. Control larvae were injected with ds-*eGFP*. qPCR was then used to measure intact and rejoined copy number of each segment in ovaries of day 1 adult females. Intact and rejoined copy number for each segment significantly differed between treatment and control ovaries (*t* test; * indicates $P \leq 0.05$; ** $P \leq 0.01$; *** $P \leq 0.001$). The *y*-axis was square root transformed to better visualize the data presented.

(Fig. S9). We also measured whether knockdown of any MdBV *vlf* or *int* family member altered amplification of proviral segments as this could also influence copy number of the intact and processed forms of each segment we measured in the preceding assay. However, knocking down these genes had no significant effect on total copy number (intact and episomal) of segments S or R (Fig. S10).

Knockdown of most late genes encoding nucleocapsid components also disables proviral segment processing

Given evidence all of the tyrosine recombinase family members detected in nucleocapsids and *p6.9-1* were required for proviral segment processing, we also asked whether normal capsid assembly was also required by knocking down each of the late genes that adversely affected capsid assembly (*vp39*, *HzNVorf9-like2*, *HzNVorf93-like*, *HzNVorf106-like*, *HzNVorf118-like*, and *27b*), followed by conducting the same qPCR assays used to assess proviral segment processing. Results showed that knockdown of each of these genes increased copy number of the intact form of each proviral segment while decreasing the rejoined form (Fig. 7). In contrast, knockdown of *35*a-5 and *K425_459,* which had no visible effects or nucleocapsid morphology or virion morphogenesis, had no significant effects on proviral segment processing (Fig. 7). None of these late genes, when knocked down, affected the amplification of proviral segments S or R, or transcript abundance of any of the tyrosine recombinase family members (Fig. S11 and S12). We thus concluded disruption of proviral segment processing was due to abnormal nucleocapsid formation rather than any of the late genes reducing proviral segment amplification or expression of any tyrosine recombinase family member.

DISCUSSION

Virion morphogenesis has been studied in a number of baculoviruses [summarized in references (35, 36)] and a few nudiviruses (37). Several differences in nuclear remodeling, membrane formation and egress have been noted between these families, but both the occluded form of baculoviruses and nudiviruses are similar in that they: (i) *de novo* produce envelopes in the nuclei of host cells, which is followed by (ii) the *de novo* assembly of preformed capsids that become nucleocapsids after packaging DNA, and (iii) envelopment of one or more nucleocapsids that produces virions. BVs also *de novo* assemble envelopes and capsids in calyx cells, but produce much higher densities of virions that unlike baculoviruses and nudiviruses fully fill the nucleus before cell lysis (27, 38–40). The focus of this study was to further characterize several of the MdBV genes encoding nucleocapsid components. While some of these genes are shared with baculoviruses, most are known only from nudiviruses and/or other BVs. We assumed several of these genes are required for assembly of capsids with a barrel-shaped morphology that all BVs produce (27, 38–40). However, we also studied several genes detected in nucleocapsids that we hypothesized are important for processing amplified proviral segments and packaging processed DNA segments into capsids. Among these, we were particularly interested in the five MdBV tyrosine site-specific recombinase family members, because two of these genes have intact catalytic domains but three do not, and *p6.9-1* because of the known requirement for this DNA binding protein in baculoviruses for genome packaging into capsids (14). The overall findings reported in this study are summarized in Fig. S13.

Like baculoviruses and presumptively nudiviruses, MdBV genes with known or hypothesized functions in virion morphogenesis are transcribed in temporally ordered cascades (14, 20, 27). Early products like the RNA polymerase subunits produce a holoenzyme that specifically transcribes some of the BV genes exhibiting late expression profiles (20). Most baculovirus genes encoding nucleocapsid components including *vlf-1* and *p6.9* are classified as late genes (14, 41, 42). Most of the MdBV genes encoding nucleocapsid components that we examined in this study also exhibit intermediate or late gene expression profiles with the exception of *vlf-1a* whose early gene expression

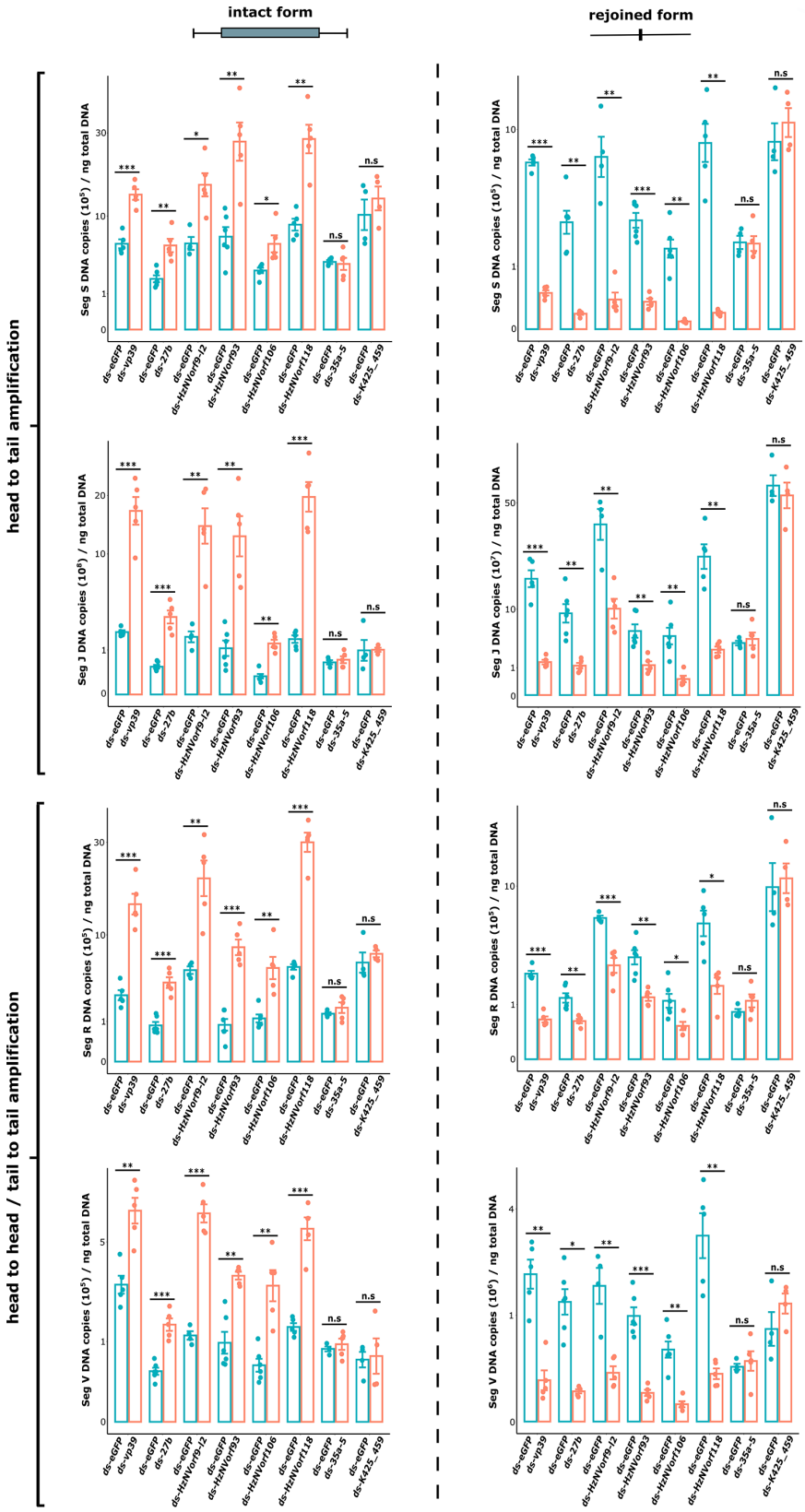

FIG 7 RNAi knockdown of late MdBV genes encoding nucleocapsid genes also alters processing of proviral segments S, J, R, or V. *M. demolitor* larvae were injected with double stranded RNA targeting *vp39, 27b*, *HzNVorf9-like2*, *HzNVorf93-like*, *HzNVorf106-like*, *HzNVorf118-like*, *35*a-5, and *K425_459*. Control

(Continued on next page)

FIG 7 (Continued)

larvae were injected with ds-*eGFP*. qPCR was then used to measure intact and rejoined copy number of each segment in ovaries of day 1 adult females. Intact and rejoined copy number for each segment significantly differed between treatment ovaries from females injected *vp39, 27b*, *HzNVorf9-like2*, *HzNVorf93-like*, *HzNVorf106-like*, or *HzNVorf118-like*, and control ovaries (*t* test; * indicates $P \leq 0.05$; ** $P \leq 0.01$; *** $P \leq 0.001$). In contrast, no differences were detected between treatment ovaries injected with *35a-5*, or *K425_459* and control ovaries (*t* test; n.s indicates $P > 0.05$). The *y*-axis was square root transformed to better visualize the data presented.

profile suggests it may have functions early in the replication cascade that we did not examine in this study.

Our RNAi assays coupled with TEM analysis indicate most of the single-copy genes encoding nucleocapsid components (*vp39*, *HzNVorf9-like2*, *HzNVorf93-like*, *HzNVorf106-like*, *HzNVorf118-like*, and *27b*) are required for assembly of capsids with a normal morphology. We earlier reported that RNAi knockdown of *vp39* reduces the number of MdBV virions in calyx cell nuclei while also increasing the sensitivity of packaged DNAs to DNase treatment (20). However, we did not note that capsid morphology was altered, which we focused on in this study. We report that *vp39* knockdown produces aberrantly shaped capsids that envelopes surround. However, we also observed many envelopes without nucleocapsids in calyx cell nuclei when *vp39* was knocked down, which is consistent with earlier results that also detected fewer nucleocapsid-containing virions when *vp39* was knocked down (20). VP39 is one of the most abundant proteins in baculovirus nucleocapsids and *Tiplua oleracea* nudivirus virions (43, 44), but few studies have characterized defects associated with its loss outside of results showing that it reduces the production of *Bombyx mori* nucleopolyhedrovirus (BmNPV) in cultured cells (45). Mutation of a single essential amino acid in *vp39* from BmNPV also reduces virus growth, while TEM data indicate this mutant results in formation of aberrant nucleocapsid-like structures (46, 47). Results from this study indicate that VP39, HzNVORFf9-like-2, HzNVORF106-like, HzNVORF118-like, and 27b are all required for assembly of MdBV capsids, which suggests that they are also likely required by nudiviruses. In contrast, our results do not identify a requirement for *35*a-5 or *K425-459* in capsid assembly. As earlier noted, *35a* has diversified into a large, 14-member family in *M. demolitor* of which three (*35a-4*, *-5*, and *-13*) encode proteins that are preferentially detected in nucleocapsids, while seven (*35a-2*, *-7*, *-8*, *-10*, *-11*, *-12*, and -14) are detected in envelopes and nucleocapsids (23). That knockdown of *35a-5* has no effect on virion morphogenesis could thus be due to redundancy, but conducting knockdown studies on all *35a* family members either alone or in combination to assess function and potential redundancies was not feasible given the large number of other genes we characterized in this study. Thus, disentangling the potential function(s) of the *35a* gene family will require a focused effort in a future investigation. In contrast, the distinct phenotype associated with knockdown of *HzNVorf9-like2* indicates this gene is not redundant with *HzNVorf9-like1*, while the still unknown function of *K425-459* is likely not involved in capsid assembly given it is a single-copy gene.

Among all of the single-copy genes we studied, knockdown of *HzNVorf93-like* generated the most unusual phenotype: formation of granular aggregations in phase 2 calyx cells that form in proximity to envelopes and nucleocapsids. Although variable in size, these granular aggregations are much smaller and morphologically distinct from nuclear chromatin or virogenic stroma as shown in Fig. S2A. BVs produced by wasps in the genus *Cotesia* have virions that contain multiple nucleocapsids (16, 38) but these also share no resemblance to the small aggregations that form after *HzNVorf93-like* knockdown, which contain no nucleocapsids but are enveloped, or the large aggregations that contain electron dense and electron translucent capsids that are not enveloped. The large aggregations containing capsids do superficially resemble occlusion bodies (OBs) that baculoviruses and some nudiviruses produce (14, 15, 48–50) but differ in that: (i) baculovirus/nudivirus OBs form late in the infection cycle, and (ii) BV producing

wasps like *M. demolitor* do not encode a polyhedrin/granulin gene which is the primary component of OBs (13, 14, 50). Alternatively, MdBV virions normally contain material between the envelope and nucleocapsid that is less electron dense than nucleocapsids containing DNA. We thus speculate the aggregations that form when we knocked down *HzNVorf93-like* is potentially the over-accumulation of this electron dense material. However, future studies will be needed to characterize the composition of this material and understand the role of HzNVORF93-like in its formation.

Deletion of *vlf-1* or *p6.9* from baculovirus genomes results in capsids that are both morphologically aberrant and electron translucent due to the absence of a packaged viral genome (14, 25, 26, 33, 34, 36). Results from this study do not detect any adverse effect of knocking down *vlf-1a*, *vlf-1b-1*, *vlf-1b-2*, *int-1*, *or p6.9-1* on MdBV capsid morphology, but loss of each does result in formation of electron translucent capsids that strongly suggest the circular DNAs that are normally packaged after processing from amplified proviral segments are absent. Our results indicate knockdown of each late gene that is required for normal capsid assembly (*HzNVorf9-like-2*, *HzNVorf93-like*, *HzNVorf106-like*, *HzNVorf118-like*, *27b*, and *vp39*) also disables proviral segment processing. Baculovirus P6.9 binds the viral genome after dephosphorylation which is required for DNA packaging (26, 51). Results from this study in turn suggest binding of dephosphorylated MdBV P6.9-1 may be required for both proviral segment processing by tyrosine site-specific recombinase family members and packaging of processed segments into capsids given knockdown of *p6.9-1* disabled both processes. Baculovirus P6.9 also undergoes phosphorylation and dephosphorylation cycles mediated in part by another core gene product conserved in BVs (38K) (12, 13, 16, 17, 26, 51), while deletion of baculovirus 38K adversely affects capsid assembly (52). We did not examine MdBV 38K in this study because we did not detect this protein in nucleocapsids (23), but we think it is likely also required for function of MdBV P6.9.1. That only two MdBV tyrosine site-specific recombinase family members have conserved catalytic domains (VLF-1a and INT-1) indicates VLF-1b-1 and VLF-1b-2 may not be functional recombinases but are nonetheless required for proviral segment processing. Our finding that VLF paralogs without conserved catalytic pentads also exist in a number of nudiviruses further suggest these non-catalytic family members may function as accessory proteins that interact with family members that have functional catalytic domains to process proviral segments. Tyrosine site-specific recombinases from other organisms have also been identified that require accessory proteins for normal function although none are non-functional family members (53, 54). Finally, our results suggest baculoviruses, nudiviruses, and BV tyrosine site-specific recombinases likely require normally assembled capsids for function given knockdown of several MdBV capsid components also disables proviral segment processing.

Prior studies show that some but not all of the circular dsDNAs BVs packaged into capsids share a conserved motif that identifies segments that integrate into the genome of infected host cells (55–57). The tyrosine site-specific recombinase family members present in BV virions and encoded by the hosts of microgastroid wasps have been suggested to catalyze the integration of these segments into the host genome (55, 58). However, evidence from this study shows that RNAi knockdown of MdBV tyrosine site-specific recombinase family members normally present in nucleocapsids inhibits proviral segment processing and packaging. It is thus possible that reduced integration into the genome of hosts is potentially due to most virions lacking packaged DNAs rather than disabling the tyrosine site-specific recombinase family members that are in nucleocapsids. Thus, additional studies are likely needed to better understand the role of BV and host-produced tyrosine recombinases in integration of circularized BV segments in the genomes of infected host cells.

In summary, by concurrently studying most of the genes encoding MdBV nucleocapsid components, we show that multiple products interact to produce capsids, process proviral segments, and package circular ds DNAs into capsids before being surrounded by envelopes to produce virions. Most of the genes of previously unknown

function that we analyzed are only known from nudiviruses or other BVs. Most of the single-copy genes we studied indicate they are required for normal capsid assembly. In contrast, most of the tyrosine site-specific recombinase family members and *p6.9-1* are required for proviral segment processing and packaging. However, our results also indicate nucleocapsids with a normal morphology are also required for proviral segment processing and packaging due presumptively to the tyrosine site-specific recombinases and P6.9-1 requiring capsids for normal function. We further hypothesize most if not all of the genes we studied have similar functions in nudiviruses. Our results do not indicate that tyrosine site-specific recombinases in MdBV nucleocapsids are differentially involved in processing proviral segments that form different concatemeric intermediates. All proviral segments are therefore likely processed by a common mechanism that involves the binding of tyrosine site-specific recombinases to motifs that identify the excision boundaries present on all the proviral segments (20–22). Finally, *Alphanudivirus* genomes that integrated into two other lineages of parasitoids have led to these wasps producing VLPs that females inject into hosts (5, 59, 60). VLPs contain nudivirus-like envelopes and capsid proteins but do not package DNA like BVs. The absence of *p6.9*, *vlf*, and *int* genes in VLP-producing wasps due to loss from the virus ancestor combined with VLPs morphologically sharing some features with MdBV virions when *p6.9-1*, *int-1*, and all of the *vlf* family members are knocked down thus also supports the essential role of these genes in BVs producing virions that transfer virulence gene-encoding DNAs to hosts.

MATERIALS AND METHODS

Insects

M. demolitor and its host *C. includens* were reared at 27 ± 1°C with a 16-h light:8-h dark photoperiod as previously described (28). *C. includens* larvae were fed an artificial diet while adults were maintained in plastic containers covered with cheese cloth and fed 10% sucrose in water. Female moths laid eggs on the cheese cloth cover and cheese-cloth strips that were in the containers. *M. demolitor* was reared by allowing females to parasitize second-third instar *C. includens* larvae from which offspring emerged and spun cocoons 7 days post-parasitism. Adult wasps were maintained in plastic containers and fed a 10% honey solution diluted in sterile water.

RNAi knockdown and quantification of target gene transcript abundance

RNAi assays were performed as detailed by Burke et al. (20). Briefly, forward and reverse primers with added T7 promoter adaptors were designed for dsRNA synthesis to the fourteen MdBV genes examined in the study (Table S1) using cDNA prepared from day 1 adult wasp ovaries with Superscript III (Invitrogen) as template and the MegaScript RNAi Kit (Ambion). Resulting 300–400 bp dsRNA products or ds-*eGFP* (control) were individually injected into the abdomen of *M. demolitor* fourth instars after completing cocoon spinning (=stage 1) at a volume of 0.5–1 µL with dsRNA concentration adjusted to 400–500 ng per µL. After emerging as adults (day 1), the paired ovaries were explanted in phosphate-buffered saline (PBS) by dissection. One ovary was removed at the lateral oviduct for use in TEM and proviral segment analysis (see below), while total RNA was extracted from the other using the QuickRNA Mini-prep kit (Zymo) to assess knockdown of the targeted gene. Total RNA was synthesized into cDNA which was used as template in qRT-PCR assays that used primers corresponding to 100–200 bp regions of each targeted gene (Table S2). Each PCR product was cloned into pSC-A-amp/kan that was Sanger sequenced to confirm identity and used to generate an absolute standard curve by serially diluting the plasmid (10^2 to 10^7 copies) using the Rotor-Gene SYBR Green PCR kit and specific qPCR primers (Table S2). Copy number of each transcript from treatment samples was determined by fitting the qRT-PCR data to the standard curve. For each gene, at least three females were examined (i.e., three biological replicate), while each

qRT-PCR assay was run in quadruplicate (four technical replicates). For statistical analysis, copy number of each gene was compared between females that were injected with ds-RNA to the target gene versus females that were injected with *eGFP* (control) using a two-tailed unpaired *t* test. Statistical analyses were performed using R (R-Project.org) with a *P* value ≤ 0.05 considered significant.

Transmission electron microscopy

Electron microscopy sample preparation was performed as earlier described (23, 27). For each RNAi knockdown treatment, the second ovary not used for total RNA isolation (see above) was fixed in 3% glutaraldehyde in phosphate buffer (pH 7.0) at 4°C. Fixed ovaries were rinsed with buffer and post-fixed using 1% osmium tetroxide. Ovaries were block stained using 0.5% uranyl acetate before being dehydrated in graded ethanol solutions, 100% acetone, and 100% propylene oxide, which was then followed by embedding in Spurr's resin. Ovaries were thin-sectioned using an ultramicrotome, mounted on copper grids, and post-stained with uranyl acetate and lead citrate. Samples were then examined using JEM-1011 Transmission Electron Microscope, equipped with an XR80M Wide-Angle Multi-Discipline Mid-Mount CCD Camera from AMT (Advanced Microscopy Techniques).

Sequence analysis of tyrosine site-specific recombinase family members

Tyrosine site-specific recombinase family members encoded by nudivirus and bracovirus genomes were manually curated or identified using PSI-BLAST with representative nudivirus integrase or VLF-1 sequences. Sequences were aligned using muscle v.3.8.31 and visualized with Jalview (61, 62). After trimming the alignment with TrimAl (-gappyout setting), a maximum likelihood phylogenetic tree was constructed with RAxML with default settings within the CIPRES Science Gateway Portal and viewed with FigTree (63–65).

DNA extraction from wasp ovaries and qPCR analysis

Wasp ovary DNA was used to quantify copy number of intact or rejoined proviral segments after RNAi knockdown of different genes was extracted using a phenol:chloroform method (20). In brief, one ovary from specific *ds-RNA* injected wasp larvae was dissected from the corresponding 1-day-old adult female within PBS (the other ovary was used for RNA extraction in order to confirm knockdown efficiency, see above). The ovary was then manually ground using a sterile pestle, followed by RNase A treatment (33 ng per µL). Ovary samples were then phenol:chloroform extracted, followed by precipitation of nucleic acids using 0.3 M sodium acetate, 25 µg of glycogen, and 100% isopropanol. Samples were rinsed with 70% ethanol, centrifuged, and solubilized in 50 µL of nuclease-free water. qPCR primers were designed to specifically target the proviral (intact), episomal and rejoined forms of four MdBV proviral segments (S, R, J, and V) (Table S3; Fig. S8). Standard curves were generated to quantify copy number for the proviral and rejoined forms of segments S, R, J, and V and the proviral and episomal forms for segment S and R (Table S3; Fig. S8). qPCR was performed using a Rotor-Gene Q (Qiagen) from which DNA gene copy numbers were obtained from four technical replicates. Copy numbers from technical replicates were then averaged to calculate copy number values for biological samples by fitting the data to standard curves generated from cloned fragments as earlier described (29). Each biological replicate represents an individual wasp sample. For statistical analyses, comparison of means between ds-*eGFP* (control) and ds-*RNA* injected female groups was tested using a two-tailed unpaired *t* test. Statistical analyses were performed by using R, with a *P* value ≤ 0.05 considered significant.

ACKNOWLEDGMENTS

The authors thank Jena Johnson for assistance with insect rearing and Mary Ard for assistance with sample processing for TEM.

This work was supported by the US Department of Agriculture (GEO00772), US National Science Foundation (DEB-1916788), and the Pulliam Endowment.

AUTHOR AFFILIATION

[1]Department of Entomology, University of Georgia, Athens, Georgia, USA

PRESENT ADDRESS

Michael J. Arvin, Human Environment and Transport Inspectorate (ILT), The Hague, Netherlands

AUTHOR ORCIDs

Gaelen R. Burke http://orcid.org/0000-0003-3472-0420
Michael R. Strand http://orcid.org/0000-0003-1844-7460

FUNDING

Funder	Grant(s)	Author(s)
U.S. Department of Agriculture (USDA)	GEO00772	Michael R. Strand
National Science Foundation (NSF)	DEB-1916788	Gaelen R. Burke

AUTHOR CONTRIBUTIONS

Ange Lorenzi, Conceptualization, Formal analysis, Investigation, Methodology, Writing – original draft, Writing – review and editing | Michael J. Arvin, Investigation, Writing – review and editing | Gaelen R. Burke, Conceptualization, Formal analysis, Funding acquisition, Investigation, Methodology, Supervision, Writing – review and editing | Michael R. Strand, Conceptualization, Formal analysis, Funding acquisition, Investigation, Methodology, Project administration, Supervision, Writing – original draft, Writing – review and editing

ADDITIONAL FILES

The following material is available online.

Supplemental Material

Table S1 to S3, Fig. S1 to S13 (JVI00817-23-s0001.pdf). Supplemental tables and figures.

REFERENCES

1. Katzourakis A, Gifford RJ, Malik HS. 2010. Endogenous viral elements in animal genomes. PLoS Genet 6:e1001191. https://doi.org/10.1371/journal.pgen.1001191
2. Holmes EC. 2011. The evolution of endogenous viral elements. Cell Host Microbe 10:368–377. https://doi.org/10.1016/j.chom.2011.09.002
3. Feschotte C, Gilbert C. 2012. Endogenous viruses: insights into viral evolution and impact on host biology. Nat Rev Genet 13:283–296. https://doi.org/10.1038/nrg3199
4. Frank JA, Feschotte C. 2017. Co-option of endogenous viral sequences for host cell function. Curr Opin Virol 25:81–89. https://doi.org/10.1016/j.coviro.2017.07.021
5. Drezen JM, Bézier A, Burke GR, Strand MR. 2022. Bracoviruses, ichnoviruses, and virus-like particles from parasitoid wasps retain many features of their virus ancestors. Curr Opin Insect Sci 49:93–100. https://doi.org/10.1016/j.cois.2021.12.003
6. Burke GR. 2019. Common themes in three independently derived endogenous nudivirus elements in parasitoid wasps. Curr Opin Insect Sci 32:28–35. https://doi.org/10.1016/j.cois.2018.10.005
7. Whitfield JB. 2002. Estimating the age of the polydnavirus/braconid wasp symbiosis. Proc Natl Acad Sci U S A 99:7508–7513. https://doi.org/10.1073/pnas.112067199
8. Bézier A, Annaheim M, Herbinière J, Wetterwald C, Gyapay G, Bernard-Samain S, Wincker P, Roditi I, Heller M, Belghazi M, Pfister-Wilhem R, Periquet G, Dupuy C, Huguet E, Volkoff A-N, Lanzrein B, Drezen J-M. 2009. Polydnaviruses of braconid wasps derive from an ancestral nudivirus. Science 323:926–930. https://doi.org/10.1126/science.1166788

9. Thézé J, Bézier A, Periquet G, Drezen J-M, Herniou EA. 2011. Paleozoic origin of insect large dsDNA viruses. Proc Natl Acad Sci U S A 108:15931–15935. https://doi.org/10.1073/pnas.1105580108
10. Bézier A, Thézé J, Gavory F, Gaillard J, Poulain J, Drezen JM, Herniou EA. 2015. The genome of the nucleopolyhedrosis-causing virus from Tipula oleracea sheds new light on the *Nudiviridae* family. J Virol 89:3008–3025. https://doi.org/10.1128/JVI.02884-14
11. Murphy N, Banks JC, Whitfield JB, Austin AD. 2008. Phylogeny of the parasitic microgastroid subfamilies (Hymenoptera: braconidae) based on sequence data from seven genes, with an improved time estimate of the origin of the lineage. Mol Phylogenet Evol 47:378–395. https://doi.org/10.1016/j.ympev.2008.01.022
12. Burke GR, Walden KKO, Whitfield JB, Robertson HM, Strand MR. 2014. Widespread genome reorganization of an obligate virus mutualist. PLoS Genet 10:e1004660. https://doi.org/10.1371/journal.pgen.1004660
13. Burke GR, Walden KKO, Whitfield JB, Robertson HM, Strand MR. 2018. Whole genome sequence of the parasitoid wasp *Microplitis demolitor* that harbors an endogenous virus mutualist. G3 (Bethesda) 8:2875–2880. https://doi.org/10.1534/g3.118.200308
14. Rohrmann GF. 2019. Baculovirus molecular biology. 4th ed. National Center for Biotechnology Information (US), Bethesda (MD).
15. Petersen JM, Bézier A, Drezen J-M, van Oers MM. 2022. The naked truth: an updated review on nudiviruses and their relationship to bracoviruses and baculoviruses. J Invertebr Pathol 189:107718. https://doi.org/10.1016/j.jip.2022.107718
16. Gauthier J, Boulain H, van Vugt J, Baudry L, Persyn E, Aury J-M, Noel B, Bretaudeau A, Legeai F, Warris S, et al. 2021. Chromosomal scale assembly of parasitic wasp genome reveals symbiotic virus colonization. Commun Biol 4:940. https://doi.org/10.1038/s42003-021-02480-9
17. Mao M, Strand MR, Burke GR. 2022. The complete genome of *Chelonus insularis* reveals dynamic arrangement of genome components in parasitoid wasps that produce bracoviruses. J Virol 96:e0157321. https://doi.org/10.1128/JVI.01573-21
18. Lorenzi A, Strand MR, Burke GR, Volkoff AN. 2022. Identifying bracovirus and ichnovirus genes involved in virion morphogenesis. Curr Opin Insect Sci 49:63–70. https://doi.org/10.1016/j.cois.2021.11.006
19. Strand MR, Burke GR. 2014. Polydnaviruses: nature's genetic engineers. Annu Rev Virol 1:333–354. https://doi.org/10.1146/annurev-virology-031413-085451
20. Burke GR, Thomas SA, Eum JH, Strand MR, Schneider DS. 2013. Mutualistic polydnaviruses share essential replication gene functions with pathogenic ancestors. PLoS Pathog 9:e1003348. https://doi.org/10.1371/journal.ppat.1003348
21. Louis F, Bézier A, Periquet G, Ferras C, Drezen J-M, Dupuy C. 2013. The bracovirus genome of the parasitoid wasp *Cotesia congregata* is amplified within 13 replication units, including sequences not packaged in the particles. J Virol 87:9649–9660. https://doi.org/10.1128/JVI.00886-13
22. Burke GR, Simmonds TJ, Thomas SA, Strand MR. 2015. *Microplitis demolitor* bracovirus proviral Loci and clustered replication genes exhibit distinct DNA amplification patterns during replication. J Virol 89:9511–9523. https://doi.org/10.1128/JVI.01388-15
23. Arvin MJ, Lorenzi A, Burke GR, Strand MR. 2021. MdBVe46 is an envelope protein that is required for virion formation by *Microplitis demolitor* bracovirus. J Gen Virol 102:001565. https://doi.org/10.1099/jgv.0.001565
24. Tweeten KA, Bulla LA, Consigli RA. 1980. Characterization of an extremely basic protein derived from granulosis virus nucleocapsid. J Virol 33:866–876. https://doi.org/10.1128/JVI.33.2.866-876.1980
25. Wang M, Tuladhar E, Shen S, Wang H, van Oers MM, Vlak JM, Westenberg M. 2010. Specificity of baculovirus P6.9 basic DNA-binding proteins and critical role of the C-terminus in virion formation. J Virol 84:8821–8828. https://doi.org/10.1128/JVI.00072-10
26. Lai Q, Wu W, Li A, Wang W, Yuan M, Yang K. 2018. The 38K-mediated specific dephosphorylation of the viral core protein P6.9 plays an important role in the nucleocapsid assembly of Autographa californica multiple nucleopolyhedrovirus. J Virol 92:e01989-17. https://doi.org/10.1128/JVI.01989-17
27. Burke GR, Strand MR. 2012. Deep sequencing identifies viral and wasp genes with potential roles in replication of *Microplitis demolitor* bracovirus. J Virol 86:3293–3306. https://doi.org/10.1128/JVI.06434-11
28. Strand MR, Johnson JA, Culin JD. 1988. Developmental interactions between the parasitoid *Microplitis demolitor* (Hymenoptera: braconidae) and its host heliothis virescens (Lepidoptera: noctuidae). Ann Entomol Soc Am 81:822–830. https://doi.org/10.1093/aesa/81.5.822
29. Beck MH, Inman RB, Strand MR. 2007. *Microplitis demolitor* bracovirus genome segments vary in abundance and are individually packaged in virions. Virology 359:179–189. https://doi.org/10.1016/j.virol.2006.09.002
30. Strand MR, McKenzie DI, Grassl V, Dover BA, Aiken JM. 1992. Persistence and expression of *Microplitis demolitor* polydnavirus in pseudoplusia includens. J Gen Virol 73 (Pt 7):1627–1635. https://doi.org/10.1099/0022-1317-73-7-1627
31. Nunes-Düby SE, Kwon HJ, Tirumalai RS, Ellenberger T, Landy A. 1998. Similarities and differences among 105 members of the *int* family of site-specific recombinases. Nucleic Acids Res 26:391–406. https://doi.org/10.1093/nar/26.2.391
32. Jayaram M, Ma C-H, Kachroo AH, Rowley PA, Guga P, Fan H-F, Voziyanov Y, Rice P, Craig N. 2015. An overview of tyrosine site-specific recombination: from an Flp perspective. Microbiol Spectr 3. https://doi.org/10.1128/microbiolspec.MDNA3-0021-2014
33. Vanarsdall A.L, Okano K, Rohrmann GF. 2004. Characterization of a baculovirus with a deletion of vlf-1. Virology 326:191–201. https://doi.org/10.1016/j.virol.2004.06.003
34. Vanarsdall Adam L., Okano K, Rohrmann GF. 2006. Characterization of the role of very late expression factor 1 in baculovirus nucleocapsid structure and DNA processing. J Virol 80:1724–1733. https://doi.org/10.1128/JVI.80.4.1724-1733.2006
35. Blissard GW, Theilmann DA. 2018. Baculovirus entry and egress from insect cells. Annu Rev Virol 5:113–139. https://doi.org/10.1146/annurev-virology-092917-043356
36. Zhao S, He G, Yang Y, Liang C. 2019. Nucleocapsid assembly of baculoviruses. Viruses 11:595. https://doi.org/10.3390/v11070595
37. Velamoor S, Mitchell A, Humbel BM, Kim W, Pushparajan C, Visnovsky G, Burga LN, Bostina M, Moscona A. 2020. Visualizing nudivirus assembly and egress. mBio 11:e01333-20. https://doi.org/10.1128/mBio.01333-20
38. Stoltz DB, Vinson SB. 1979. Viruses and parasitism in insects. Adv Virus Res 24:125–171. https://doi.org/10.1016/s0065-3527(08)60393-0
39. Strand MR. 1994. *Microplitis demolitor* polydnavirus infects and expresses in specific morphotypes of pseudoplusia includens haemocytes. J Gen Virol 75 (Pt 11):3007–3020. https://doi.org/10.1099/0022-1317-75-11-3007
40. Wyler T, Lanzrein B. 2003. Ovary development and polydnavirus morphogenesis in the parasitic wasp *Chelonus inanitus*. II. Ultrastructural analysis of calyx cell development, virion formation and release. J Gen Virol 84:1151–1163. https://doi.org/10.1099/vir.0.18830-0
41. Wilson ME, Mainprize TH, Friesen PD, Miller LK. 1987. Location, transcription, and sequence of a baculovirus gene encoding a small arginine-rich polypeptide. J Virol 61:661–666. https://doi.org/10.1128/JVI.61.3.661-666.1987
42. McLachlin JR, Miller LK. 1994. Identification and characterization of vlf-1, a baculovirus gene involved in very late gene expression. J Virol 68:7746–7756. https://doi.org/10.1128/jvi.68.12.7746-7756.1994
43. Hou D, Zhang L, Deng F, Fang W, Wang R, Liu X, Guo L, Rayner S, Chen X, Wang H, Hu Z. 2013. Comparative proteomics reveal fundamental structural and functional differences between the two progeny phenotypes of a baculovirus. J Virol 87:829–839. https://doi.org/10.1128/JVI.02329-12
44. Bézier A, Harichaux G, Musset K, Labas V, Herniou EA. 2017. Qualitative proteomic analysis of Tipula oleracea nudivirus occlusion bodies. J Gen Virol 98:284–295. https://doi.org/10.1099/jgv.0.000661
45. Ono C, Kamagata T, Taka H, Sahara K, Asano S, Bando H. 2012. Phenotypic grouping of 141 BmNPVs lacking viral gene sequences. Virus Res 165:197–206. https://doi.org/10.1016/j.virusres.2012.02.016
46. Li Y, Wang J, Deng R, Zhang Q, Yang K, Wang X. 2005. Vlf-1 deletion brought AcMNPV to defect in nucleonucleocapsid formation. Virus Genes 31:275–284. https://doi.org/10.1007/s11262-005-3242-3
47. Katsuma S, Kokusho R. 2017. A conserved glycine residue is required for proper functioning of a baculovirus VP39 protein. J Virol 91:e02253-16. https://doi.org/10.1128/JVI.02253-16
48. Chaivisuthangkura P, Tawilert C, Tejangkura T, Rukpratanporn S, Longyant S, Sithigorngul W, Sithigorngul P. 2008. Molecular isolation

and characterization of a novel occlusion body protein gene from penaeus monodon nucleopolyhedrovirus. Virology 381:261–267. https://doi.org/10.1016/j.virol.2008.08.036
49. Raina AK, Adams JR, Lupiani B, Lynn DE, Kim W, Burand JP, Dougherty EM. 2000. Further characterization of the gonad-specific virus of corn earworm, *Helicoverpa zea*. J Invertebr Pathol 76:6–12. https://doi.org/10.1006/jipa.2000.4942
50. Yang Y-T, Lee D-Y, Wang Y, Hu J-M, Li W-H, Leu J-H, Chang G-D, Ke H-M, Kang S-T, Lin S-S, Kou G-H, Lo C-F. 2014. The genome and occlusion bodies of marine penaeus monodon nudivirus (PmNV), also known as MBV and PemoNPV, suggest that it should be assigned to a new nudivirus genus that is distinct from the terrestrial nudiviruses. BMC Genomics 15:628. https://doi.org/10.1186/1471-2164-15-628
51. Li A, Zhao H, Lai Q, Huang Z, Yuan M, Yang K. 2015. Posttranslational modifications of baculovirus protamine-like protein P6.9 and the significance of its hyperphosphorylation for viral very late gene hyperexpression. J Virol 89:7646–7659. https://doi.org/10.1128/JVI.00333-15
52. Wu W, Lin T, Pan L, Yu M, Li Z, Pang Y, Yang K. 2006. Autographa californica multiple nucleopolyhedrovirus assembly is interrupted upon deletion of the 38k gene. J Virol 80:11475–11485. https://doi.org/10.1128/JVI.01155-06
53. Gourlay SC, Colloms SD. 2004. Control of Cre recombination by regulatory elements from Xer recombination systems. Mol Microbiol 52:53–65. https://doi.org/10.1111/j.1365-2958.2003.03962.x
54. Grainge I, Pathania S, Vologodskii A, Harshey RM, Jayaram M. 2002. Symmetric DNA sites are functionally asymmetric within Flp and Cre site-specific DNA recombination synapses. J Mol Biol 320:515–527. https://doi.org/10.1016/s0022-2836(02)00517-x
55. Beck MH, Zhang S, Bitra K, Burke GR, Strand MR. 2011. The encapsidated genome of *Microplitis demolitor* bracovirus integrates into the host pseudoplusia Includens. J Virol 85:11685–11696. https://doi.org/10.1128/JVI.05726-11
56. Chevignon G, Periquet G, Gyapay G, Vega-Czarny N, Musset K, Drezen J-M, Huguet E. 2018. *Cotesia congregata* bracovirus circles encoding PTP and ankyrin genes integrate into the DNA of parasitized manduca sexta hemocytes. J Virol 92:e00438-18. https://doi.org/10.1128/JVI.00438-18
57. Muller H, Chebbi MA, Bouzar C, Périquet G, Fortuna T, Calatayud P-A, Le Ru B, Obonyo J, Kaiser L, Drezen J-M, Huguet E, Gilbert C. 2021. Genome-wide patterns of bracovirus chromosomal integration into multiple host tissues during parasitism. J Virol 95:e0068421. https://doi.org/10.1128/JVI.00684-21
58. Wang Z, Ye X, Zhou Y, Wu X, Hu R, Zhu J, Chen T, Huguet E, Shi M, Drezen J-M, Huang J, Chen X, Palli SR. 2021. Bracoviruses recruit host integrases for their integration into caterpillar's genome. PLoS Genet 17:e1009751. https://doi.org/10.1371/journal.pgen.1009751
59. Pichon A, Bézier A, Urbach S, Aury J-M, Jouan V, Ravallec M, Guy J, Cousserans F, Thézé J, Gauthier J, Demettre E, Schmieder S, Wurmser F, Sibut V, Poirié M, Colinet D, da Silva C, Couloux A, Barbe V, Drezen J-M, Volkoff A-N. 2015. Recurrent DNA virus domestication leading to different parasite virulence strategies. Sci Adv 1:e1501150. https://doi.org/10.1126/sciadv.1501150
60. Burke GR, Simmonds TJ, Sharanowski BJ, Geib SM. 2018. Rapid viral symbiogeensis via changes in parasitoid wasp genome architecture. Mol Biol Evol 35:2463–2474. https://doi.org/10.1093/molbev/msy148
61. Edgar RC. 2004. MUSCLE: multiple sequence alignment with high accuracy and high throughput. Nucleic Acids Res 32:1792–1797. https://doi.org/10.1093/nar/gkh340
62. Waterhouse AM, Procter JB, Martin DMA, Clamp M, Barton GJ. 2009. Jalview version 2 – a multiple sequence alignment editor and analysis workbench. Bioinformatics 25:1189–1191. https://doi.org/10.1093/bioinformatics/btp033
63. Capella-Gutiérrez S, Silla-Martínez JM, Gabaldón T. 2009. trimAL: a tool for automated alignment trimming in large-scale phylogenetic analyses. Bioinformatics 25:1972–1973. https://doi.org/10.1093/bioinformatics/btp348
64. Stamatakis A. 2014. RAxML version 8: a tool for phylogenetic analysis and post-analysis of large phylogenies. Bioinformatics 30:1312–1313. https://doi.org/10.1093/bioinformatics/btu033
65. Miller MA, Pfeiffer W, Schwartz T. 2010. Creating the CIPRES science gateway for inference of large phylogenetic trees. Proceedings of the gateway computing environments workshop (GCR), p 1–8. IEEE New Orleans. https://doi.org/10.1109/GCE.2010.5676129